J Biol Inorg Chem (2010) 15:967–976
DOI 10.1007/s00775-010-0658-6

ORIGINAL PAPER

A new CuZ active form in the catalytic reduction of N_2O by nitrous oxide reductase from *Pseudomonas nautica*

Simone Dell'Acqua · Sofia R. Pauleta · Patrícia M. Paes de Sousa · Enrico Monzani · Luigi Casella · José J. G. Moura · Isabel Moura

Received: 19 January 2010 / Accepted: 4 April 2010 / Published online: 27 April 2010

Abstract The final step of bacterial denitrification, the two-electron reduction of N_2O to N_2, is catalyzed by a multi-copper enzyme named nitrous oxide reductase. The catalytic centre of this enzyme is a tetranuclear copper site called CuZ, unique in biological systems. The in vitro reconstruction of the activity requires a slow activation in the presence of the artificial electron donor, reduced methyl viologen, necessary to reduce CuZ from the resting non-active state ($1Cu^{II}/3Cu^{I}$) to the fully reduced state ($4Cu^{I}$), in contrast to the turnover cycle, which is very fast. In the present work, the direct reaction of the activated form of *Pseudomonas nautica* nitrous oxide reductase with stoichiometric amounts of N_2O allowed the identification of a new reactive intermediate of the catalytic centre, CuZ°, in the turnover cycle, characterized by an intense absorption band at 680 nm. Moreover, the first mediated electrochemical study of *Ps. nautica* nitrous oxide reductase with its physiological electron donor, cytochrome *c*-552, was performed. The intermolecular electron transfer was analysed by cyclic voltammetry, under catalytic conditions, and a second-order rate constant of $(5.5 \pm 0.9) \times 10^5\ M^{-1}\ s^{-1}$ was determined. Both the reaction of stoichiometric amounts of substrate and the electrochemical studies show that the active CuZ° species, generated in the absence of reductants, can rearrange to the resting non-active CuZ state. In this light, new aspects of the catalytic and activation/inactivation mechanism of the enzyme are discussed.

Keywords Nitrous oxide reductase · Catalytic mechanism · Denitrification · Bioelectrochemistry

Electronic supplementary material The online version of this article (doi:10.1007/s00775-010-0658-6) contains supplementary material, which is available to authorized users.

S. Dell'Acqua · S. R. Pauleta · P. M. Paes de Sousa · J. J. G. Moura · I. Moura (✉)
REQUIMTE/CQFB,
Departamento de Química,
Faculdade de Ciências e Tecnologia,
Universidade Nova de Lisboa,
2829-516 Caparica, Portugal
e-mail: isa@dq.fct.unl.pt

S. Dell'Acqua · E. Monzani · L. Casella
Dipartimento di Chimica Generale,
Università di Pavia,
Via Taramelli 12,
27100 Pavia, Italy

Introduction

The multi-copper enzyme nitrous oxide reductase (N_2OR) catalyzes the final step of bacterial dissimilatory denitrification ($2NO_3^- \rightarrow 2NO_2^- \rightarrow 2NO \rightarrow N_2O \rightarrow N_2$), namely the two-electron reduction of the kinetically inert molecule nitrous oxide (N_2O) to dinitrogen (N_2) and water [1, 2].

Recently, the structure of N_2OR from *Pseudomonas nautica* [3], *Paracoccus denitrificans* [4] and *Achromobacter cycloclastes* [5] was solved. The crystal structure revealed that N_2OR is a functional homodimer containing two different multi-copper centres per subunit, called CuA and CuZ.

The binuclear copper centre, CuA, is an electron transfer centre similar to the CuA found in cytochrome oxidases and its properties have been extensively studied [6–9]. CuZ is a novel mixed-valence copper centre (Cu_4S) with a sulfide ion bridging a distorted tetrahedron of copper atoms, a unique structural feature in biology. This cluster is coordinated by seven histidines, and a water-derived ligand is proposed to bridge the two copper ions (CuI and CuIV), where the substrate binds to the enzyme.

The CuZ from *Ps. nautica* N_2OR, in the as-isolated state, contains a $1Cu^{II}/3Cu^{I}$ redox state with a total spin of ½, where the unpaired electron is delocalized between two or more copper atoms through the bridging sulfide ion [10–12]. This state, which has a typical electronic spectral band at 640 nm and a four-line splitting EPR signature [13, 14], cannot be easily reduced or oxidized. The catalytically active, fully reduced form ($4Cu^{I}$) can be obtained only after a prolonged incubation with reduced methyl viologen (MV) [15, 16].

In contrast, the catalytic centre, CuZ, of *Pa. denitrificans* N_2OR has been identified in two forms, named CuZ and CuZ*, with the relative proportion between them depending on the purification conditions [17]. In particular, the CuZ* form, characterized by an intense absorption band at 650 nm, is more abundant in the 'aerobic' preparation, whereas the CuZ form, with an absorption band at 670 nm, is predominant in the 'anaerobic' preparation. CuZ* is redox-inert, whereas the CuZ midpoint potential was calculated to be $E^{\circ\prime} = 60$ mV (vs. the standard hydrogen electrode). Despite this feature, the 'aerobic' preparation shows a slightly higher steady-state activity compared with the 'anaerobic' preparation. In addition, the CuZ form has an EPR spectrum similar to that of the CuZ* form, suggesting a $1Cu^{II}/3Cu^{I}$ redox state for both species [17].

Recently, the catalytic parameters of *Ps. nautica* N_2OR activity were determined to compare the physiological (*Ps. nautica* cytochrome *c*-552) and artificial (MV) electron donors [18]. This study revealed that these two electron donors have a distinct mechanism of interaction towards the enzyme, whereas when cytochrome *c*-552 was used as an electron donor, $k_{cat} = 3.8\ s^{-1}$, $K_m = 50.2\ \mu M$ and $pK_a = 8.3$ were estimated, and when an artificial electron donor, MV, was used, $k_{cat} = 320\ s^{-1}$, $K_m = 11.5\ \mu M$ and $pK_a = 6.6$ were obtained.

We present here the first mediated electrochemical study of N_2OR with its physiological electron donor, cytochrome *c*-552. The electrochemical behaviour of this cytochrome has been well characterized [19], and it has already been shown to be the electron donor of other enzymes isolated from *Ps. nautica*, cytochrome *c* peroxidase [20] and cytochrome cd_1 nitrite reductase [21]. In the latter case the electron transfer reaction was also investigated using electrochemical techniques.

To understand the complex mechanism of activation and catalysis of N_2OR CuZ, we have also studied the properties of the enzyme in the activated form by direct reaction of N_2OR with stoichiometric amounts of substrate in the absence of reductants. The identification of a new active intermediate of the catalytic centre, CuZ°, led us to revise both the catalytic and the activation mechanism of this challenging enzyme.

Materials and methods

Protein purification

N_2OR was purified from *Ps. nautica* 617 (also known as *Marinobacter hydrocarbonoclasticus* 617) cellular extract as previously described [13], with some minor modifications. Enzyme concentrations were determined by the Lowry method [22].

Ps. nautica cytochrome *c*-552 was purified as previously described [23], with some minor modifications. The concentration of cytochrome *c*-552 was determined spectrophotometrically using the extinction coefficient at 552 nm, $\varepsilon = 19.3\ mM^{-1}\ cm^{-1}$ [24], for the fully reduced form.

Enzyme activation and activity assay

Enzyme activation was performed in a glove box as previously described [18]. The activity assay used was the one described in [18], using MV as the electron donor.

Electrochemical methods

Voltammetric measurements were performed using an AUTOLAB/PSTAT 12 potentiostat/galvanostat from ECO Chemie (Utrecht, The Netherlands). Data were analysed with the GPES software package from ECO Chemie. A conventional three-electrode-configuration cell was used, with a platinum auxiliary electrode and a saturated calomel reference electrode [+244 mV vs. the standard hydrogen electrode (SHE)]. The working electrode was a pyrolytic graphite electrode, with a diameter of 3 mm (surface area 0.07 cm^2), which was used in a membrane configuration [19]. Throughout the paper, all potentials are referred to the SHE.

Before each experiment, the pyrolytic graphite electrode was polished by hand on a polishing cloth (Buehler 40-7212) using a water–alumina slurry (0.05 μm, Buehler 40-6365-006), sonicated for 5 min and rinsed carefully with Milli-Q water. The membrane electrode was prepared by dropping a 5-μl drop, containing 2.5 μM preactivated N_2OR and 50 μM oxidized cytochrome *c*-552, on a small square (10 mm × 10 mm) of negatively charged Spectra/Por MWCO 3500 dialysis membrane. The membrane was fitted tightly to the electrode with a rubber O-ring.

In typical experiments, the working solution contained 0.1 M phosphate buffer pH 7.0, the scan rate was 40 mV s^{-1}, and cyclic voltammograms were obtained in the range from +0.6 to −0.25 V versus the SHE.

For the scan-rate dependence of the catalytic current, cyclic voltammograms were obtained between 5 and 100 mV s^{-1}. In the determination of the N_2O concentration dependence of the catalytic current, 8, 17, 25, 33, 48,

125, 330 and 1,000 μM N_2O were added as N_2O-saturated water. In the pH-dependence studies of the catalytic current, the following buffers were used: 0.1 M potassium phosphate buffer at pH 5.9, 6.2, 6.4, 6.7 and 7.0, or 0.1 M tris(hydroxymethyl)aminomethane (Tris)–HCl at pH 7.3, 7.6, 8.0, 8.4 and 8.8. All the electrochemical experiments were performed inside a glove box filled with an argon-saturated atmosphere.

Direct reaction of N_2OR with substrate

For the direct reaction of the enzyme with substrate, an equimolar amount of N_2O was added to 35 μM N_2OR preactivated in 0.1 M Tris–HCl at pH 7.6. The reaction was followed using a TIDAS diode-array spectrophotometer. At corresponding incubation times, an aliquot of this solution was taken to determine the enzyme activity, using MV reduced with sodium dithionite as an electron donor, as previously described [18].

EPR spectroscopy

X-band EPR spectra were recorded using a Bruker EMX spectrometer equipped with a rectangular cavity (model ER4102ST) and an Oxford Instruments continuous-flow cryostat. EPR spectra were simulated using the program WINEPR Simfonia version 1.2 from Bruker Instruments.

The sample of the enzyme form characterized by the 680-nm absorption band was prepared under anaerobic conditions (glove box) by mixing 75 μM preactivated N_2OR and an equimolar amount of N_2O, in 0.1 M Tris–HCl. The EPR tube was frozen with liquid nitrogen 1 min after the addition of N_2O. The resting CuZ form, with absorption at 640 nm, was obtained by exposing the previous sample to air for 30 min. The experimental conditions are described in the legend for Fig. 6.

Redox titration

Preactivated N_2OR (35 μM) in 0.1 M Tris–HCl pH 7.6 was titrated in a 1-ml cuvette. The potential was measured with a platinum–silver/silver chloride combined electrode (Crison). The oxidation experiments were performed with addition of potassium ferricyanide ($E = +420$ mV vs. SHE) and the reaction was followed by the UV–vis spectra. The reduction experiments were performed with addition of sodium dithionite or titanium(III) citrate and the reaction was also followed by the UV–vis spectra. The following mediators were added, each at 2 μM concentration: 1,2-naphthoquinone-4-sulfonic acid, 1,2-naphthoquinone, phenazine methosulfate, resorufin (2,8-dihydroxyphenoxazine), indigodisulfonate, 2-hydroxy-1,4-naphthoquinone and MV. The titration was performed in a glove box.

Results and discussion

Electrocatalytic activity of *Ps. nautica* N_2OR with cytochrome *c*-552 as an electron donor

The catalytic activity of *Ps. nautica* N_2OR for N_2O reduction was analysed for the first time by mediated electrochemistry using *Ps. nautica* cytochrome *c*-552, a small electron transfer protein that was established to be the physiological redox partner of this enzyme [18]. For this purpose, both redox partners were entrapped between the electrode surface and a dialysis membrane [25] and cyclic voltammetry was performed.

In the absence of cytochrome *c*-552, preactivated or non-pre-activated N_2OR does not exhibit any electrochemical signal, probably owing to the non-compatibility of the negatively charged graphite electrode surface and the negatively charged surface of *Ps. nautica* N_2OR (pI = 5.4). Moreover, no catalytic current was observed in these conditions upon addition of nitrous oxide to preactivated N_2OR within the potential range used.

In previous reports, cytochrome *c*-552 was shown to exhibit a well-defined direct electrochemical signal at a carbon membrane electrode [19]. In our experimental conditions, this reversible electrochemical behaviour was also verified and the calculated redox potential, $E^{\circ\prime} = +(245 \pm 5)$ mV versus the SHE at pH 7, is in agreement with the one reported in that study. In our work, although the membrane configuration was used, the peak currents of cytochrome *c*-552 varied linearly with the square root of the scan rate, as expected for a diffusion-controlled process, a behaviour that has also been observed in other studies for this type of protein with this electrode configuration [26].

The cyclic voltammograms of cytochrome *c*-552 alone (data not shown) and the ones in the presence of preactivated N_2OR are identical (Fig. 1, continuous line). Upon addition of a saturating amount of substrate, N_2O, the original peak-shaped voltammogram transforms into the characteristic sigmoid catalytic wave, with a steady-state current plateau (Fig. 1, dashed line).

This behaviour can be interpreted with the reaction mechanism shown in Scheme 1. An initial heterogeneous electron transfer reaction at the electrode (step 1) is followed by two homogeneous chemical reactions: the reduced form of cytochrome *c*-552 is oxidized by N_2OR (step 2), which is then regenerated by N_2O (step 3).

This mechanism can be simplified to

$$\text{cytochrome } c_{552ox} + e^- \rightleftarrows \text{cytochrome } c_{552red} \quad (1)$$

$$\text{cytochrome } c_{552red} + N_2OR_{ox} \rightarrow \text{cytochrome } c_{552ox} + N_2OR_{red} \quad (2)$$

$$N_2OR_{red} + N_2O \rightarrow N_2OR_{ox} + N_2 \quad (3)$$

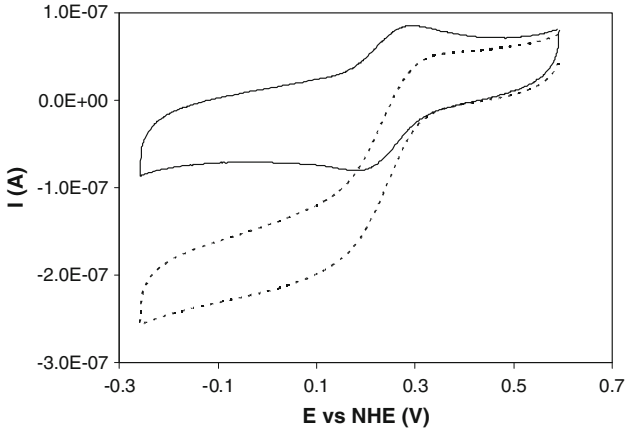

Fig. 1 Cyclic voltammograms (40 mV s^{-1}) of 50 μM cytochrome *c*-552 entrapped in a membrane electrode with 2.5 μM activated *Pseudomonas nautica* nitrous oxide reductase (N_2OR), in 0.1 M phosphate buffer, pH 7. The *continuous line* is the cyclic voltammogram in the absence of substrate and the *dashed line* is the cyclic voltammogram after addition of 1 mM N_2O. *NHE* normal hydrogen electrode

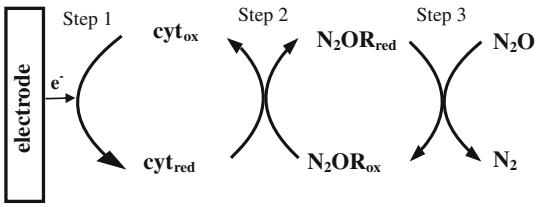

Scheme 1 Mediation scheme for N_2OR: the electrode reduces cytochrome *c*-552, which is immediately reoxidized by N_2OR; the level of oxidized N_2OR is then restored by conversion of N_2O to N_2

as long as four conditions are obeyed: (1) the heterogeneous electron transfer (step 1) is a reversible reaction; (2) the homogeneous chemical reaction (step 2) is irreversible; (3) the reaction between cytochrome *c*-552 and N_2OR is pseudo-first order with the reaction rate constant given by $k' = k[N_2OR]$, where k is the second-order rate constant; (4) reaction 3 is fast.

As reported in [19] and confirmed in this work, the first condition is verified. The experiments were performed under an excess of the substrate N_2O; thus, the enzyme is reoxidized by the catalytic reaction (step 3), and not by transferring electrons back to cytochrome *c*-552. For this reason, the second condition is obeyed. Condition 3 implies that the enzyme concentration is much higher than that of cytochrome *c*-552. Although this is not the case, the saturating concentration of N_2O guarantees that the oxidized form of the enzyme is quickly restored by step 3, as long as the latter is not rate-limiting (condition 4). Therefore, N_2OR will always be available to react with cytochrome *c*-552 and pseudo-first-order conditions are met.

According to the theory of steady-state voltammetric catalysis, the rate constant can only be determined from the steady-state catalytic current if the latter is not scan-rate-dependent [27, 28]. For the mediated catalysis of N_2OR by cytochrome *c*-552, the catalytic current increases linearly with the scan rate, between 5 and 40 mV s^{-1}, and then becomes independent of this parameter, up to 100 mV s^{-1} (data not shown). Moreover, the catalytic current decreases after the first scan, until the initial cytochrome *c*-552 signal is restored. This behaviour, corroborated by the fact that further addition of substrate does not restore the catalytic signal, suggests that the enzyme is being inactivated (see below).

The rate constant of the intermolecular electron transfer reaction between cytochrome *c*-552 and N_2OR was estimated using two approaches, with the catalytic currents being measured at 40 mV s^{-1}. In one of the approaches, the cyclic voltammetry data were processed according to the Nicholson and Shain theory [27], where the pseudo-first-order rate constant, k', can be determined by plotting the ratio between the catalytic current (the plateau current value, i_{cat}) and the diffusion-controlled current (the cytochrome *c*-552 reduction peak current, i_p) versus the reciprocal of the square root of the scan rate, v:

$$i_{cat}/i_p = 2.241(RT/nF)^{1/2}k'^{1/2}(1/v)^{1/2}, \quad (1)$$

where n is the number of electrons exchanged, and R, T and F are the universal gas constant, the temperature, and the Faraday constant, respectively. The cytochrome *c*-552 redox reaction is a reversible one-electron process, and thus from the slope a k' value of 1.4 ± 0.2 s^{-1} was obtained. The intermolecular rate constant, k, for the reaction between N_2OR and cytochrome *c*-552 at pH 7.0 was determined to be $(5.4 \pm 0.8) \times 10^5$ M^{-1} s^{-1}, since the concentration of enzyme entrapped in the membrane was 2.5 μM.

In the other approach, k is calculated from the value of the N_2O-saturated limiting current, i_{cat} [29–32]:

$$i_{cat} = nFAC_{\text{cytochrome } c}\left(D_{\text{cytochrome } c}k'\right)^{1/2}, \quad (2)$$

where $C_{cyt\ c}$ is the concentration of cytochrome *c*-552 under the membrane, $D_{cyt\ c}$ is its diffusion coefficient (1.0×10^{-6} cm^2 s^{-1} [33]) and A is the electrode surface area (see "Materials and methods"). Calculations with this equation gave $k = (5.6 \pm 0.4) \times 10^5$ M^{-1} s^{-1} at pH 7.0, a value identical to the one obtained with the previous approach (Eq. 1).

This value compares well with other intermolecular rate constants determined using cyclic voltammetry. Cytochrome *c*-552 was used in mediated electrochemical experiments for the reduction of nitrite by *Ps. nautica* cytochrome cd_1 nitrite reductase [21] and a similar rate constant was calculated in that study [$k = (4.1 \pm 0.1) \times 10^5$ M^{-1} s^{-1} at pH 6.3]. Other examples are the electron transfer from *A. cycloclastes* pseudoazurin to its electron donor, nitrite

reductase, which was determined to have a k value of 7.3×10^5 M^{-1} s^{-1} [34], and also the electron transfer between *Paracoccus pantotrophus* pseudoazurin and cytochrome *c* peroxidase, with $k = 1.4 \times 10^5$ M^{-1} s^{-1} [25].

This voltammetric theory implies that the catalytic current should be directly proportional to the mediator concentration. This condition is verified because the electrochemical experiments were performed with 50 μM, corresponding to the linear region of the Michaelis–Menten equation ($K_{mc-552} = 50\,\mu M$ [18]). However, investigation of the catalytic current at higher cytochrome *c*-552 concentrations revealed a non-linear behaviour (data not shown), confirming that also cytochrome *c*-552 contributes to the global rate with a Michaelis–Menten term [18].

It is possible to compare the second-order kinetic constant, k, calculated with the electrochemical approach [$k = (5.5 \pm 0.9) \times 10^5$ M^{-1} s^{-1}] with the ratio k_{cat}/K_m determined by the steady-state kinetic study [$(7.6 \pm 0.7) \times 10^4$ M^{-1} s^{-1}; see the electronic supplementary material]. The difference between the two values can be attributed to the limitations of the steady-state kinetic study, where k_{cat} and K_m were not determined accurately owing to experimental problems at high cytochrome *c*-552 concentrations [18].

The dependence of the electrochemical activity on the nitrous oxide concentration was studied using constant concentrations of N_2OR and cytochrome *c*-552 entrapped in the membrane. The catalytic currents calculated for each substrate concentration were fitted to the Michaelis–Menten equation (Fig. 2), using a K_m of (16 ± 2) μM and an i_{catmax} of $(3.9 \pm 0.1) \times 10^{-7}$ A.

K_{mN_2O}, with cytochrome *c*-552 as an electron donor, could not be estimated in the steady-state activity assay because the N_2O reduction is involved in a fast step compared with the N_2OR reduction by cytochrome *c*-552 [18]. The value obtained in that study using MV as an electron donor (($K_{mN_2O} = 14.0 \pm 2.9\,\mu M$)) is very similar to the one calculated by steady-state kinetics, but it must be pointed out that when a stationary electrode is used, mass transport limitations are not avoided at low substrate concentrations. Therefore, the K_m value estimated from the fitting of the electrochemical assay should not be regarded as accurate, whereas from the i_{catmax} value it was possible to calculate a k'_{max} value of (1.4 ± 0.1) s^{-1}. Since the N_2OR concentration used in this study was 2.5 μM, a k of $(5.6 \pm 0.4) \times 10^5$ M^{-1} s^{-1} was estimated, a value that is identical to the one calculated using the approaches presented above.

The effect of pH on the intermolecular rate constant was analysed, revealing a bell-shaped curve, that can be simulated using Eq. 3 [35] and pK_a values of 5.5 ± 1.0 and 8.0 ± 0.7 (Fig. 3).

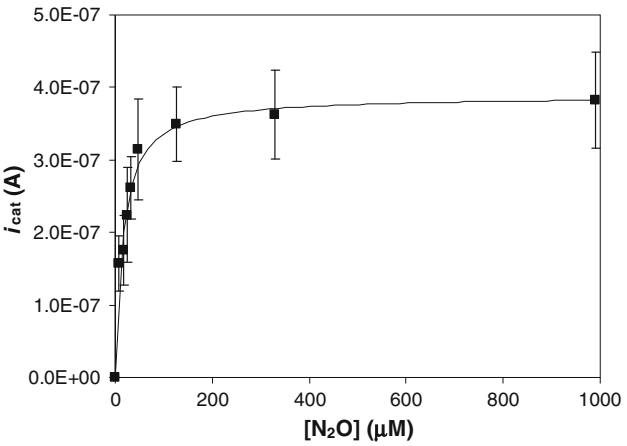

Fig. 2 Catalytic current from electrochemical assays of *Ps. nautica* N_2OR using cytochrome *c*-552 as a mediator versus N_2O concentration. The assays were performed with 2.5 μM activated N_2OR and 50 μM cytochrome *c*-552 entrapped in the membrane electrode, in 0.1 M phosphate buffer at pH 7, and in the presence of 8, 17, 25, 33, 48, 125, 330 and 1,000 μM N_2O-saturated water. The experimental data were fitted with the Michaelis–Menten equation, using a K_m of (16 ± 2) μM and an i_{catmax} of $(3.9 \pm 0.1) \times 10^{-7}$ A

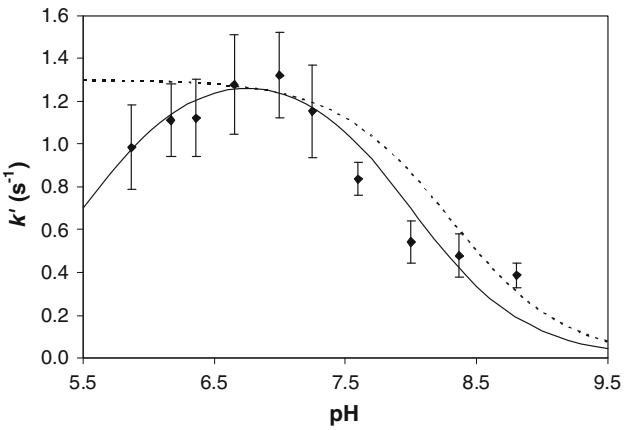

Fig. 3 Intermolecular rate constants of *Ps. nautica* N_2OR versus pH, determined by electrochemical assays using cytochrome *c*-552 as a mediator. The assays were performed with 2.5 μM activated N_2OR and 50 μM cytochrome *c*-552 entrapped in the membrane electrode, 1 mM N_2O-saturated water, in different buffer systems with pH between 5.9 and 8.8. The data were non-linearly fitted using Eq. 3, and pK_a values of 8.0 ± 0.7 and 5.5 ± 1.0 (*solid line*). The *dashed line* shows the pH-dependence fit for the steady-state kinetic study [18], with a pK_a of 8.3

$$\mathrm{Act} = \mathrm{Act}_{max} \Big/ \left(1 + 10^{(pK_{a1} - pH)} + 10^{(pH - pK_{a2})}\right) \quad (3)$$

The latter pK_a matches the solution kinetic value (pK_a of 8.3 [18]), which was attributed to a deprotonation occurring at the catalytic CuZ centre and identified as a key process in the reduction mechanism of CuZ. The more acidic pK_a was not detected in the steady-state kinetic experiment, since it is outside the pH range studied in that work (pH between 6.2 and 8.7).

As mentioned above, in the electrochemical studies of the mediated activity of N_2OR by cytochrome *c*-552 it was observed that the catalytic current, measured at successive scans, decreases after each scan (Fig. 5b, filled circles). This decay can be attributed to an inactivation process that occurs with time (between each new scan). Moreover, in the experiments performed at different pH, it was observed that this inactivation process is lower at acidic pH than at basic pH (Fig. 4), and a pK_a of 7.1 ± 0.8 was estimated. This is an indication that a deprotonation is involved in the inactivation of the enzyme (vide infra), as has been proposed before [18].

Direct reaction with substrate N_2O

The reaction between preactivated N_2OR and a stoichiometric amount of N_2O, monitored by UV–vis spectroscopy, showed a rapid (within 1 s) oxidation of the CuA centre, through the increase of the two characteristic absorption bands at 480 and 540 nm [13], and the development of an absorption band at 680 nm, which has not been reported previously. Then, this 680-nm absorption band slowly (on the order of minutes) shifts to the usual position of 640 nm for the resting enzyme (Fig. 5a). At times corresponding to those in the UV–vis monitoring, the enzyme activity was assayed to understand the contribution to catalysis of the N_2OR forms characterized by the 680-nm absorption band and the form featuring the 640-nm absorption band (Fig. 5b).

The increase of the intensity of 640-nm band in the UV–vis spectrum versus time (Fig. 5b, open squares) can be fitted with a rate similar to the decay rate of the enzymatic activity (Fig. 5b, filled squares) ($k = 0.3$ min^{-1} for both experimental data sets), suggesting that the two processes are directly correlated.

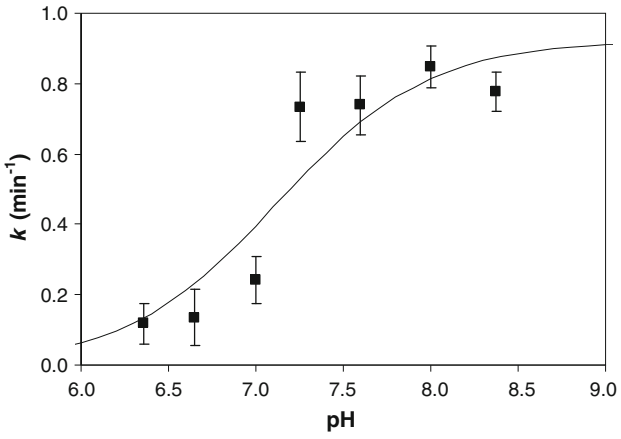

Fig. 4 Rate constant of the inactivation process detected by electrochemical experiments versus pH. The *k* values were obtained by fitting the catalytic current decay with an exponential equation. The data were non-linearly fitted using Eq. 3 adapted for one pK_a of 7.1

The maximum activity for this enzyme preparation determined in a separate activity assay was 133 μmol N_2O/min mg N_2OR. The activity calculated 1 min after the reaction between N_2OR and a stoichiometric amount of N_2O is 130 μmol N_2O/min mg N_2OR (98% with respect to the initial value). The activity decreases with time, reaching a value of 0.6 μmol N_2O/min mg N_2OR (0.4% with respect to the initial value) after 48 min.

The direct correlation of the enzyme activity (Fig. 5b, filled squares) with the presence of a N_2OR form exhibiting the 680-nm band (Fig. 5b, open circles) indicates that CuZ is in a new redox-active form, which will be represented here as CuZ°. This also rules out that the broad 680-nm

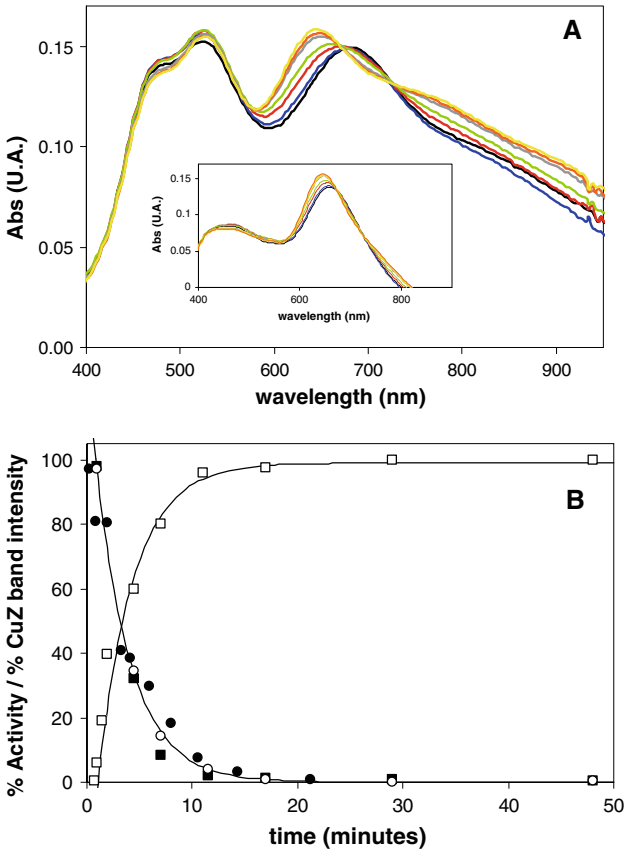

Fig. 5 **a** Selected spectra of 35 μM *Ps. nautica* N_2OR after reaction with an equimolar amount of N_2O at the following times: 0.5 min (*black*), 1 min (*blue*), 1.5 min (*red*), 2 min (*green*), 4.5 min (*grey*), 11 min (*orange*) and 45 min (*yellow*). *Inset*: Spectra obtained after subtraction of the oxidized CuA contribution at the following times: 0.5 min (*black*), 1 min (*blue*), 1.5 min (*red*), 2 min (*green*), 4.5 min (*grey*), 11 min (*orange*) and 45 min (*yellow*). **b** N_2OR activity (*filled squares*) versus time (100% corresponds to 133 μmol N_2O reduced min^{-1} mg^{-1} enzyme) and 640-nm band intensity (*open squares*) versus time (100% corresponds to the final spectra at $t = 48$ min and 0% corresponds to the first spectrum at $t = 1$ min). *Solid lines* are exponential fits and $k = 0.3$ min^{-1} was used for both fits. *Filled circles* represent the percentage of electrocatalytic activity versus time (100% corresponds to the maximum activity, characterized by an intermolecular rate constant for electron transfer, k', of 1.4 s^{-1}). *Open circles* represent the 680-nm band intensity

absorption band might have a contribution from the 640-nm absorption band.

Therefore, this is the first time that such an enzyme form has been shown to be directly involved in the turnover mechanism of N_2OR. In fact, the two enzyme forms previously identified for *Pa. denitrificans* N_2OR, CuZ and CuZ*, which also have different absorption bands (670 and 650 nm, respectively), show very low specific activity when compared with the active CuZ° form [17].

The EPR spectrum of the CuZ° form was obtained by direct reaction of fully reduced N_2OR with a stoichiometric amount of N_2O for 1 min (Fig. 6). The oxidized CuA centre contributes to the total EPR spectrum with its typical seven-line hyperfine splitting [7, 36], so this contribution was subtracted in the spectra shown in Fig. 6. The resting, inactive CuZ form characterized by the band at 640 nm in the UV–vis spectrum, exhibits the following EPR parameters: $g_{\|} = 2.160$ and $g_{\perp} = 2.040$ and a four-line hyperfine splitting [10] (Fig. 6b).

The EPR signal of the active CuZ° form is very similar, both in shape and intensity (Fig. 6, spectrum a), indicating that it has the same paramagnetic state as the resting form ($1Cu^{II}/3Cu^{I}$), with a total spin $S = ½$. The $g_{\|}$ value is unchanged, whereas $g_{\perp}$ is only slightly lower ($g_{\perp} = 2.037$) for CuZ°. In light of this similarity in the EPR spectrum, the coordination environment of the coppers in the two forms has not changed drastically, and in particular we can assume that CuI remains in the formal Cu^{2+} state within the cluster [10], whereas the small change in $g_{\perp}$ may suggest that some minor local rearrangement is occurring at the site. Also the shift of the electronic band from CuZ to CuZ° can be correlated to some minor change in the CuI environment.

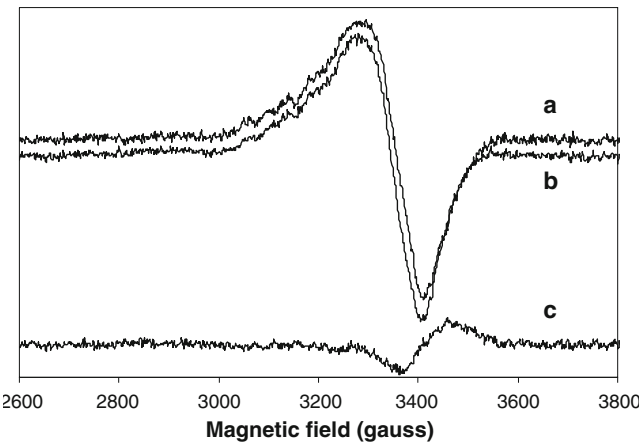

Fig. 6 EPR spectra of the different CuZ forms. EPR spectrum of the 680-nm band, CuZ° form (*a*), and of the 640-nm band, resting CuZ form (*b*). The CuA contribution was subtracted from both spectra. The difference between the spectrum of the CuZ° form and that of the resting, inactive CuZ form is shown in *c*. The instrumental parameters were as follows: modulation amplitude 5 G, microwave frequency 9.66 GHz and temperature 30 K

The high intensity of the 680-nm band in CuZ° confirms that this absorption band remains a $S^{2-} \rightarrow$ Cu ligand to metal charge transfer (LMCT) transition, as for the 640-nm band in the resting CuZ, which is actually a multicomponent band with partially overlapping features at higher and lower energy [11, 12]. Indeed, looking carefully at the difference spectra reported in the inset in Fig. 5a, it seems that the 680-nm absorption of CuZ° results from the overlap between the high-intensity component, which is red-shifted from its original position at 640 nm, and a low-intensity component, blue-shifted from its position near 720 nm, in the CuZ spectrum, which is missing in the CuZ° spectrum. The increased bandwidth of the 680-nm band with respect to the 640-nm band supports this interpretation. We may therefore interpret the 640- to 680-nm shift of the LMCT band as a result of the reduction of the splitting between the components of the complex $S^{2-} \rightarrow$ Cu LMCT band, indicating that in the CuZ° centre, the CuI atom undergoes a small displacement in its relative position versus the μ_4–S^{2-} ligand with respect to the resting CuZ cluster.

A possible explanation for the spectral difference between CuZ and CuZ° is a protonation/deprotonation process of the hydroxo ligand between CuI and CuIV. As a simple proton transfer would be faster than the timescale of conversion of CuZ° to the redox-equivalent, inactive form, it is likely that the deprotonation of a bound water molecule in CuZ° (see below) occurs with formation of a μ-hydroxo-bridge between CuI and CuIV in the resting form [18]. This will likely involve some minor structural change in the cluster to meet the geometrical requirement needed to optimize the formation of the bridge.

In a recent crystallographic study of *A. cycloclastes* N_2OR, it was shown that the CuZ cluster is flexible and can accommodate alternatively one water molecule and one hydroxyl group or even an iodide ion in a bridged mode [5]. In particular, it was shown that the CuZ cluster can rearrange its structure by changing the Cu–S distances and the orientation of some of the histidine residues. From our data we can suggest that the configuration with the μ-hydroxo bridge between CuI and CuIV prevents the CuZ centre from undergoing further catalysis, whereas a non-bridged water molecule would be more susceptible to be released, enabling the accommodation of a new substrate molecule at CuZ.

Mechanistic insight involving the new CuZ° active form

On the basis of the identification of the fast-reacting CuZ° N_2OR form, it is possible to formulate a new mechanism of

reduction, catalysis and inactivation of the catalytic N_2OR centre, as shown in Scheme 2. The resting CuZ state, characterized by the absorption band at 640 nm, does not participate in the catalytic cycle because of the slow reduction (activation process) required to obtain the fully reduced state [15]. The fast turnover cycle ($k_{cat} = 320\ s^{-1}$ and $k_{cat} = 3.8\ s^{-1}$ for MV and cytochrome *c*-552, respectively [18]) implies that the re-reduction of the N_2O-oxidized CuZ centre must be rapid in the enzymatic turnover and excludes the involvement of the resting CuZ state. This is also in agreement with the fact that as-purified N_2OR is not catalytically active, unless it is subjected to prolonged activation with reduced MV.

Therefore, the two-electron-oxidized form of CuZ is not detectable as it has a very short life and is very rapidly reduced by one electron coming from CuA, yielding the $1Cu^{2+}3Cu^{+}$ intermediate species CuZ° (Scheme 2). The intramolecular electron transfer producing CuZ° cannot be analysed in our conditions but is signalled by the formation of the characteristic optical bands of oxidized CuA (on 0.1-s timescale). Then, during catalytic turnover, CuZ° is directly reduced back to the fully reduced enzyme by another electron coming from CuA. As the enzymatic reaction produces a water molecule by consumption of two protons, we believe that this water molecule is bound to the oxidized CuI in CuZ°. The fast reduction of the latter species during turnover prevents the rearrangement of CuZ° to the μ-hydroxo-bridged, redox-equivalent resting form. We already noticed that the Cu(II)/Cu(I) redox potential of the μ-hydroxo-bridged dinuclear Cu(II) complexes is lower than that of the corresponding aqua complexes [18]. This is consistent with the formulation of the oxidized CuI–CuIV as a non-bridged $Cu^{2+}Cu^{2+}$–H_2O species, as this would make the subsequent reduction by CuA easier.

In the typical activity assays, the strong absorption of the reductants (reduced MV or cytochrome *c*-552) prevents the detection of the CuZ° intermediate form. Instead, as shown here, in the absence of reductants, this form is slowly converted to the inactive resting state of CuZ. Moreover, the inactivation process does not involve any electron transfer reaction, because CuA remains in the oxidized state ($Cu^{1.5+}/Cu^{1.5+}$) during this process.

The inactivation process that was detected in the electrochemical experiments, where the activity of N_2OR is mediated by cytochrome *c*-552, has the same decay as the one observed in the UV–vis study, which suggests that the process that is occurring is the same in the two situations. In addition, the effect of pH on the inactivation process is consistent with the deprotonation of the water ligand between CuI and CuIV in the CuZ° species, as the pK_a calculated from the inactivation process (7.1 ± 0.8) is compatible with the values calculated through the electrochemical assay and the steady-state kinetic study (p$K_a = 8.0 \pm 0.7$ and p$K_a = 8.3$, respectively)

Redox titration

The titration of N_2OR was performed in the oxidation direction since the activated form is in the fully reduced state. The CuA centre has a midpoint potential at $E \approx 240$ mV (Fig. 7, filled squares in the oxidation

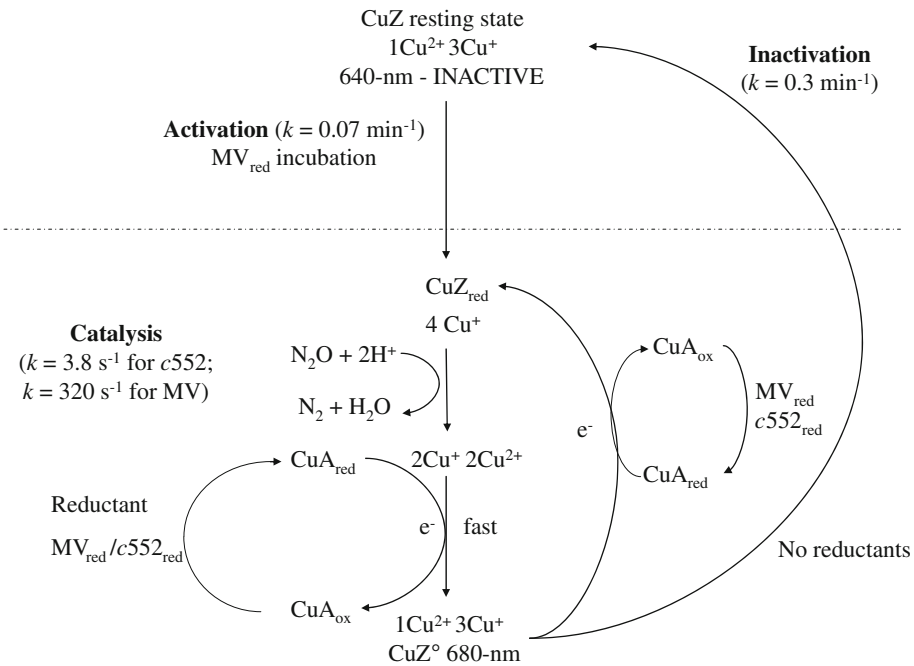

Scheme 2 New mechanism of reduction, inactivation and catalysis of the catalytic N_2OR centre, CuZ centre

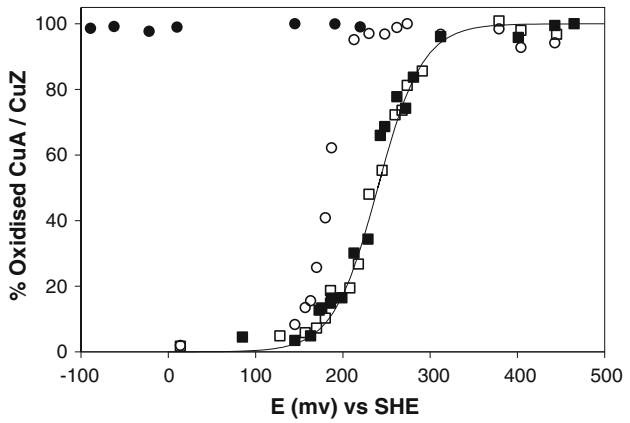

Fig. 7 Potentiometric redox titration of fully reduced *Ps. nautica* N_2OR following the characteristic absorption bands of the CuA and CuZ centres in the oxidation and reduction directions. The CuA centre was monitored by following the absorption at 540 nm in the oxidative (*filled squares*) and in the reductive (*open squares*) titrations. The titration curve was fitted with $E^{o\prime} = +240$ mV (*solid line*). The CuZ centre was monitored by following the absorption at 640 nm in the oxidative (*open circles*) and in the reductive (*filled circles*) titrations

direction, open squares in the reduction direction). This midpoint potential is in full agreement with literature values for this centre in N_2OR [13, 17, 37]. The oxidation of CuZ brings this centre directly into the form characterized by the 640-nm band with no contribution at 680 nm (Fig. 7, open circles, spectra not shown). The impossibility to reduce this form [titrations using either dithionite or titanium(III) citrate were not successful; Fig. 7, filled circles] does not allow the application of the Nernst equation, which can be used only for a reversible system, and does not enable the calculation of the midpoint redox potential for this centre. In fact, this data set does not fit with the Nernst equation for one electron.

The oxidation of the fully reduced CuZ promoted by ferricyanide brings CuZ directly into the inactive form, which is characterized by the 640-nm band. This form cannot be re-reduced again unless through an activation process with reduced MV (Scheme 2).

The irreversible oxidation of CuZ is catalytically unproductive and this behaviour confirms the proposed mechanism in which CuZ° is the only active form in the turnover cycle, where it is generated by the substrate and it is rapidly reduced by the electron flow from the CuA centre.

Conclusion

The first example of mediated electrochemistry of N_2OR described here allowed the calculation of the rate constant of the intermolecular electron transfer to the physiological electron donor [k of $(5.5 \pm 0.9) \times 10^5$ M^{-1} s^{-1}]. The rate constant is similar to the values found for other intermolecular protein–protein electron transfers determined using cyclic voltammetry. Moreover, the study of the dependence of the rate on N_2O concentration and pH confirms the recent results obtained in the kinetic analysis between N_2OR and cytochrome *c*-552 from *Ps. nautica*.

The reaction of the activated form of N_2OR with a stoichiometric amount of substrate enabled the identification of a new active CuZ° form in the turnover cycle, which is characterized by an absorption band at 680 nm and is different from the resting and inactive CuZ form, previously observed. In the absence of reductants to complete the catalytic cycle, the CuZ° form rearranges to restore the resting form in a slow process ($k = 0.3$ min^{-1}), compared with the turnover rate. This inactivation process was also detected in the electrochemical studies, where the catalytic current decreased at a rate similar to the rate of formation of the inactive enzyme form.

A scheme that shows the activation required in vitro and the inactivation detected during these experiments was presented. In particular, the difference between the resting CuZ and the active CuZ° was discussed to clarify the activation mechanism and the catalysis of N_2OR.

Acknowledgements This research was supported by FCT (Fundação para a Ciência e Tecnologia) grants PTDC/QUI/64638/2006 (to I.M.) and SFRH/BD/30414/2006 (to S.D.) and by the University of Pavia through FAR (to E.M. and L.C.). We thank Pablo J. Gonzalez for the help with EPR data collection.

References

1. Zumft WG, Kroneck PM (2007) Adv Microb Physiol 52:107–227
2. Tavares P, Pereira AS, Moura JJ, Moura I (2006) J Inorg Biochem 100:2087–2100
3. Brown K, Tegoni M, Prudencio M, Pereira AS, Besson S, Moura JJ, Moura I, Cambillau C (2000) Nat Struct Biol 7:191–195
4. Haltia T, Brown K, Tegoni M, Cambillau C, Saraste M, Mattila K, Djinovic-Carugo K (2003) Biochem J 369:77–88
5. Paraskevopoulos K, Antonyuk SV, Sawers RG, Eady RR, Hasnain SS (2006) J Mol Biol 362:55–65
6. Scott RA, Zumft WG, Coyle CL, Dooley DM (1989) Proc Natl Acad Sci USA 86:4082–4086
7. Antholine WE, Kastrau DH, Steffens GC, Buse G, Zumft WG, Kroneck PM (1992) Eur J Biochem 209:875–881
8. Gorelsky SI, Xie X, Chen Y, Fee JA, Solomon EI (2006) J Am Chem Soc 128:16452–16453
9. Kroneck PM, Antholine WA, Riester J, Zumft WG (1989) FEBS Lett 248:212–213
10. Chen P, DeBeer George S, Cabrito I, Antholine WE, Moura JJ, Moura I, Hedman B, Hodgson KO, Solomon EI (2002) J Am Chem Soc 124:744–745
11. Chen P, Cabrito I, Moura JJ, Moura I, Solomon EI (2002) J Am Chem Soc 124:10497–10507
12. Chen P, Gorelsky SI, Ghosh S, Solomon EI (2004) Angew Chem Int Ed 43:4132–4140
13. Prudencio M, Pereira AS, Tavares P, Besson S, Cabrito I, Brown K, Samyn B, Devreese B, Van Beeumen J, Rusnak F, Fauque G,

Moura JJ, Tegoni M, Cambillau C, Moura I (2000) Biochemistry 39:3899–3907
14. Oganesyan VS, Rasmussen T, Fairhurst S, Thomson AJ (2004) Dalton Trans 7:996–1002
15. Ghosh S, Gorelsky SI, Chen P, Cabrito I, Moura JJ, Moura I, Solomon EI (2003) J Am Chem Soc 125:15708–15709
16. Chan JM, Bollinger JA, Grewell CL, Dooley DM (2004) J Am Chem Soc 126:3030–3031
17. Rasmussen T, Berks BC, Butt JN, Thomson AJ (2002) Biochem J 364:807–815
18. Dell'acqua S, Pauleta SR, Monzani E, Pereira AS, Casella L, Moura JJ, Moura I (2008) Biochemistry 47:10852–10862
19. Correia dos Santos MM, Paes de Sousa PM, Simoes Gonçalves ML, Krippahl L, Moura JJG, Lojou E, Bianco P (2003) J Electroanal Chem 541:153–162
20. Alves T, Besson S, Duarte LC, Pettigrew GW, Girio FM, Devreese B, Vandenberghe I, Van Beeumen J, Fauque G, Moura I (1999) Biochim Biophys Acta 1434:248–259
21. Lopes H, Besson S, Moura I, Moura JJ (2001) J Biol Inorg Chem 6:55–62
22. Lowry OH, Rosebrough NJ, Farr AL, Randall RJ (1951) J Biol Chem 193:265–275
23. Fauque G, Moura JJG, Besson S, Saraiva L, Moura I (1992) Oceanis 18:211–216
24. Saraiva LM, Besson S, Fauque G, Moura I (1994) Biochem Biophys Res Commun 199:1289–1296
25. de Sousa PM, Pauleta SR, Goncalves ML, Pettigrew GW, Moura I, Dos Santos MM, Moura JJ (2007) J Biol Inorg Chem 12:691–698
26. Ferapontova EE, Ruzgas T, Gorton L (2003) Anal Chem 75:4841–4850
27. Nicholson RS, Shain I (1964) Anal Chem 36:706–723
28. Bard AJ, Faulkner LR (2001) Electrochemical methods, fundamentals and applications. Wiley, New York
29. Saveant JM, Vianello E (1965) Electrochim Acta 10:905–920
30. Coury LA, Oliver BN, Egekeze JO, Sosnoff CS, Brumfield JC, Buck RP, Murray RW (1990) Anal Chem 62:452–458
31. Coury LA, Yang Liu, Murray RW (1993) Anal Chem 65:242–246
32. Yang L, Coury LA, Murray RW (1993) J Phys Chem 97:1694–1700
33. Correia dos Santos MM, Paes de Sousa PM, Simoes Gonçalves ML, Lopes H, Moura I, Moura JJG (1999) J Electroanal Chem 464:76–84
34. Kataoka K, Yamaguchi K, Kobayashi M, Mori T, Bokui N, Suzuki S (2004) J Biol Chem 279:53374–53378
35. Cornish-Bowden A (2001) Fundamentals of enzyme kinetics. Portland Press, London, pp 179–192
36. Farrar JA, Thomson AJ, Cheesman MR, Dooley DM, Zumft WG (1991) FEBS Lett 294:11–15
37. Coyle CL, Zumft WG, Kroneck PM, Korner H, Jakob W (1985) Eur J Biochem 153:459–467